Human Molecular Genetics, 2005, Vol. 14, No. 13 ***1709–1725***
doi:10.1093/hmg/ddi178
Advance Access published on May 11, 2005

Cell type-specific gene expression of midbrain dopaminergic neurons reveals molecules involved in their vulnerability and protection

Chee Yeun Chung[1,2], Hyemyung Seo[1,†], Kai Christian Sonntag[1], Andrew Brooks[3], Ling Lin[1] and Ole Isacson[1,2,*]

[1]Neuroregeneration Laboratories, Harvard Medical School, McLean Hospital, 115 Mill Street, Belmont, MA 02478, USA, [2]Harvard Center for Neurodegeneration and Repair, Boston, MA 02114, USA and [3]Department of Environmental Medicine, Aab Institute of Biomedical Sciences, University of Rochester Medical Center, Rochester, NY 14642, USA

Received April 1, 2005; Revised and Accepted May 2, 2005

Molecular differences between dopamine (DA) neurons may explain why the mesostriatal DA neurons in the A9 region preferentially degenerate in Parkinson's disease (PD) and toxic models, whereas the adjacent A10 region mesolimbic and mesocortical DA neurons are relatively spared. To characterize innate physiological differences between A9 and A10 DA neurons, we determined gene expression profiles in these neurons in the adult mouse by laser capture microdissection, microarray analysis and real-time PCR. We found 42 genes relatively elevated in A9 DA neurons, whereas 61 genes were elevated in A10 DA neurons [>2-fold; false discovery rate (FDR) <1%]. Genes of interest for further functional analysis were selected by criteria of (i) fold differences in gene expression, (ii) real-time PCR validation and (iii) potential roles in neurotoxic or protective biochemical pathways. Three A9-elevated molecules [G-protein coupled inwardly rectifying K channel 2 (GIRK2), adenine nucleotide translocator 2 (ANT-2) and the growth factor IGF-1] and three A10-elevated peptides (GRP, CGRP and PACAP) were further examined in both α-synuclein overexpressing PC12 (PC12-αSyn) cells and rat primary ventral mesencephalic (VM) cultures exposed to MPP^+ neurotoxicity. GIRK2-positive DA neurons were more vulnerable to MPP^+ toxicity and overexpression of GIRK2 increased the vulnerability of PC12-αSyn cells to the toxin. Blocking of ANT decreased vulnerability to MPP^+ in both cell culture systems. Exposing cells to IGF-1, GRP and PACAP decreased vulnerability of both cell types to MPP^+, whereas CGRP protected PC12-αSyn cells but not primary VM DA neurons. These results indicate that certain differentially expressed molecules in A9 and A10 DA neurons may play key roles in their relative vulnerability to toxins and PD.

INTRODUCTION

Major unsolved problems for most neurodegenerative diseases include determining specific factors that cause relative vulnerabilities of neuronal populations. This problem is exemplified by Parkinson's disease (PD), in which there is relative vulnerability even among neighboring midbrain populations of neurons releasing the same neurotransmitter, dopamine (DA).

DA neurons in the ventral midbrain consist of two main groups: the A9 group in the substantia nigra (SN) and the A10 group in the medial and ventral tegmentum (1). A9 and A10 DA neurons project to different anatomical structures and are involved in distinct functions. A9 DA neurons mainly project to the dorsolateral striatum, involved in the control of motor functions, whereas A10 DA neurons provide connections to the ventromedial striatum, limbic and cortical regions, involved in reward and emotional behavior. In addition to the distinct axonal projections and differences in synaptic connectivity, these groups of DA neurons exhibit differences in neurochemistry and electrophysiological prop-

*To whom correspondence should be addressed. Tel: +1 6178553283; Fax: +1 6178553284; Email: isacson@hms.harvard.edu
[†]Present address: Department of Molecular and Life Science, Hanyang University, Korea

erties (2,3), illustrating the functional differences despite similar neurotransmitter identity.

The most prominent neuropathology of PD is degeneration or dysfunction of midbrain DA neurons. Most PD cases are sporadic, for which a combination of environmental and genetic factors is the proposed etiology (4,5). The remaining cases are familial PD and caused by monogenic mutations on molecules such as α-synuclein (6) ubiquitin C-terminal hydrolase-1 (7), parkin (8), DJ-1 (9) and PINK1 (10) or, in the case of α-synuclein, also by triplication of the wild-type gene (11). Strikingly, and independent of specific etiology, 9 DA neurons are preferentially affected in PD and A10 DA neurons relatively spared (12–15). Similar patterns of degeneration appear in rodents and primate models of PD (13,16,17), indicating that the physiological differences between A9 and A10 DA neurons may be conserved between species.

Postmortem analyses of human PD brains demonstrate a selective cell loss of the A9 DA neuron group with a survival rate of ∼10% (14,18–20), whereas the A10 group is largely spared with a survival rate of ∼60% even in severe cases (14,21,22). This indicates that A9 DA neurons are more vulnerable to intrinsic and/or extrinsic factors causing degeneration in PD. In addition, three regional gradients of neurodegeneration in the dorso-ventral/rostro-caudal/medio-lateral axis have been reported in PD. Caudally and laterally located ventral DA cells within A9 DA neurons are the most vulnerable cells in PD (14,15). In contrast, the medial and rostral part of DA cell subgroups within A10 DA neurons (i.e. rostral linear nucleus, RLi) are the least affected (5–25% cell loss) (14,22).

Certain proteins differentially expressed in A9 and A10 DA neurons may play critical roles in susceptibility to or protection against neurodegenerative processes in PD. Previous studies have reported several proteins that are differentially expressed in A9 and A10 DA neurons. For example, calbindin $D_{28}K$, an intracellular calcium binding protein has been used to distinguish resistant from vulnerable DA neurons in PD patient brain and animal models of PD, because it is colocalized in the resistant DA population (mostly A10 DA neurons) (23–25). Another of these proteins is G-protein-gated inwardly rectifying K^+ channel (GIRK), which generates a slow inhibitory postsynaptic potential (IPSP) in DA neurons via activation of D_2 or $GABA_B$ receptors and controls the membrane excitability of DA neurons. This can modulate the release of DA from synaptic terminals of DA neurons to the striatum. Among four isoforms of GIRK, only GIRK2 is exclusively expressed in the vulnerable DA neurons (mostly A9 neurons) (26,27), and it has been implicated in A9 DA neuron pathology in *weaver* mice (28–30).

The general hypothesis for this kind of exploration is that idiopathic, environmental and genetically driven processes culminating in neurodegenerative diseases are present in most cellular systems, but only reach a pathological threshold in very specific and characteristic neuronal populations (31,32). To determine the critical molecular differences that could result in vulnerability or provide opportunities for neuroprotection, we characterized the gene expression profiles of A9 and A10 DA neurons from adult mouse midbrain by laser capture microdissection (LCM) followed by microarray analysis and validation using real-time PCR. Some of the molecules from this analysis were then examined for functional relevance using PD-related *in vitro* cellular bioassays.

RESULTS

Gene expression profiles of A9 and A10 DA neurons based on LCM and microarray analysis

In our experiments, midbrain A9 and A10 DA neuronal groups were identified by rapid TH-immunostaining designed to minimize RNA degradation in tissue sections and microdissected by LCM using anatomical criteria (Fig. 1A–1D) as described in Materials and Methods. Using real-time PCR, we validated the quality of the extracted RNA samples by confirming the mRNA levels of GIRK2 known to be elevated in A9 DA neurons (26,27) and calbindin $D_{28}K$ known to be elevated in A10 DA neurons (23–25) (Fig. 1E). Glial fibrillary acidic protein (GFAP) was undetectable in both A9 and A10 samples, demonstrating the purity of the LCM samples (data not shown). To investigate the molecular differences between DA neurons located in the A9 and A10 midbrain regions, we performed microarray analysis to compare the gene expression profiles of A9 and A10 DA neurons. In total, five biological replicates from A9 and six biological replicates from A10 regions of mouse brain were analyzed on an Affymetrix Murine 430A high-density oligonucleotide array, which currently queries 22 000 murine probe sets. Paired hybridization results between replicates of A9 (Fig. 1F) and A10 (Fig. 1G) samples demonstrated the reproducibility between the biological replicates. The distribution of gene expression signals from the combined data of the A9 and A10 series displayed similarity and even distribution of A9-elevated and A10-elevated genes in the plot (Fig. 1H). Only a small number of genes were differentially expressed. Forty-two genes had >2.0-fold elevation of mRNA levels in A9 compared with A10 DA neurons (Table 1) and 221 genes had >1.5-fold elevation (FDR $< 1\%$) (Supplementary Material, Table S1). Sixty-one genes had >2.0-fold elevation of mRNA levels in A10 compared with A9 DA neurons (Table 1) and 167 genes had >1.5-fold elevation (FDR $< 1\%$) (Supplementary Material, Table S1). We validated the microarray analysis in two ways. First, we verified previously reported gene expression differences reported between A9 and A10 DA neurons. For example, Raldh1 (33) was elevated in A9 neurons and calbindin $D_{28}K$ (23–25) and cholecystokinin (34,35) were elevated in A10 DA neurons (Supplementary Material, Table S1). The known A9-elevated molecule, GIRK2, was confirmed only by real-time PCR as mentioned earlier [2.78-fold more expressed in A9 DA neurons (SEM $\pm$ 0.94)], because GIRK2 gene is not represented in the microarray chips used in this study. Secondly, using real-time PCR of laser-captured RNA samples, we quantified the mRNA levels of several genes from our microarray analysis to confirm gene expression patterns (Table 2). We chose to validate genes from various functional categories with potential association to relative vulnerability. Among the 16 genes tested, none failed validation by quantitative PCR. To gain insight into the biological relevance of differential A9/A10 gene expression, we analyzed genes that exhibited significant differences (FDR $< 1\%$) with Onto-Express (OE) software, which systematically translates

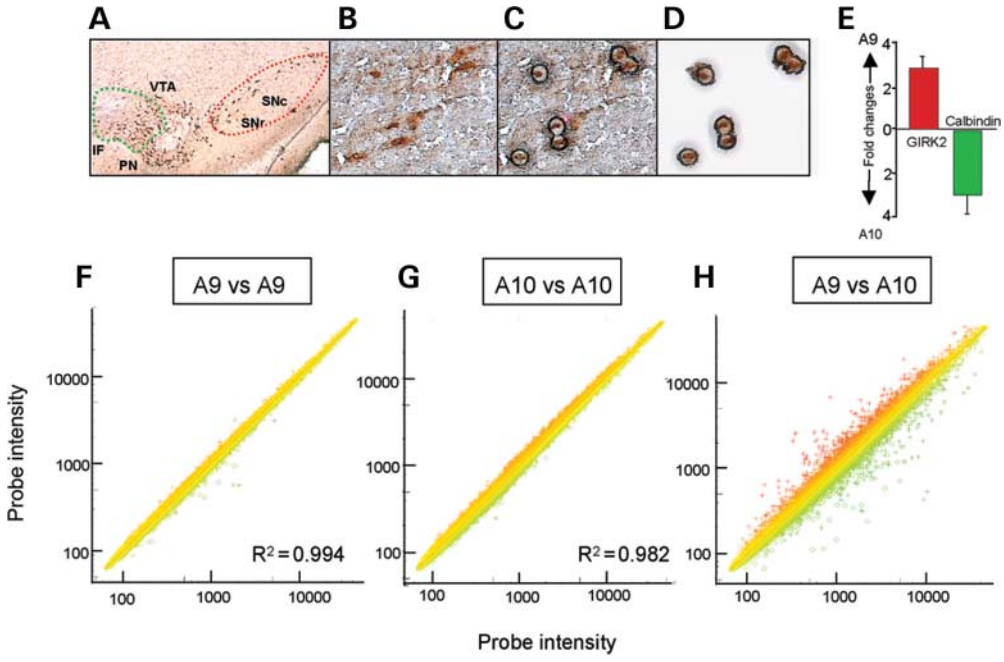

Figure 1. LCM and microarray on A9 and A10 DA neurons. (**A**) Coronal section of the mouse midbrain after quick TH immunostaining. A9 DA neurons are located in the SN pars reticulata (SNr) and the lateral part of SN pars compacta (SNc) marked by a red dotted line. A10 DA neurons are located in the medial part of the ventral tegmental area (VTA), the nucleus PN and the interfascicular nucleus (IF) marked by a green dotted line. (**B**–**D**) LCM of the midbrain DA neurons. Selection of DA neurons was guided by quick TH immunostaining. (B) TH-positive neurons in SNc before laser capture. (C) The TH-positive cells were targeted for laser capture with a 7.5 μM laser diameter. (D) Captured cells on the thermoplastic film were visualized before processing for RNA extraction. (**E**) Validation of GIRK2 and calbindin $D_{28}K$ mRNA levels in LCM samples by real-time PCR. The transcript level of GIRK2 was 2.78-fold (SEM ± 0.94) higher in A9 and that of calbindin was 2.90-fold (SEM ± 0.64) higher in A10 DA neurons. (**F** and **G**) Gene expression profiles of A9 and A10 DA neurons determined by microarray analysis. There is a high reproducibility between A9 (F) and A10 (G) microarray replicates. (**H**) Differential gene expression between A9 and A10 replicates showed genes with differential expression. All genes were plotted on a log scale and represent a comparison between microdissected samples of A9 and A10. Five A9 replicates are plotted against six A10 replicates to determine the differential gene expression between the groups. The distance from the midline infers increasing levels of differential gene expression. All data were normalized using the probe level Robust Multi-Chip Analysis (RMA) algorithm.

genetic input into functional profiles (36). Genes from several categories showed interesting differences among cell groups. Genes related to metabolism (Fig. 2A) and genes encoding mitochondrial proteins (Fig. 2B) were elevated in A9 DA neurons compared with A10 DA neurons. Genes involved in protein, lipid and vesicle-mediated transport, but not ion transport, were also elevated in A9 DA neurons (Fig. 2C). Several genes related to small GTPase-mediated signaling and synaptic vesicle recycling, including RAB and RAS proteins (37), were elevated in A9 DA neurons (Supplementary Material, Table S1) and genes related to neuropeptide and hormone activity and axon guidance were elevated in A10 cells (Table 3). Intriguingly, certain opposing molecular functional categories exhibited inverse expression patterns in A9 and A10 DA neurons. For example, gene expression of proteases and phosphatases was elevated in A9 DA neurons, whereas inhibitors of proteases and phosphatases were elevated in A10 DA neurons (Table 3). Two pro-apoptotic genes, caspase 7 and Bcl2-like 11 (38), were elevated in A9 neurons (Table 3).

Altered vulnerability of α-synuclein overexpressing PC12 cells and primary VM cultures by molecules elevated in A9 DA neurons

To investigate and to efficiently screen candidate genes with functional relevance to PD-related vulnerability, we used inducible α-synuclein overexpressing PC12 cells (PC12-αSyn) (39) in combination with MPP^+ treatment. This cell culture model combines two features of PD-related pathogenetic mechanisms: MPP^+-induced mitochondrial complex I inhibition (40) and α-synuclein overexpression (11). We first established that overexpression of α-synuclein increased the susceptibility of PC12 cells to MPP^+. There were 32% (SEM ± 2.6), 66% (SEM ± 3.8) and 20% (SEM ± 3.8) increases in LDH release at 1, 2.5, and 5 mM MPP^+, respectively, when compared with control PC12 cells ($P < 0.05$; $n = 4$). We then investigated GIRK2, which is known to be elevated in A9 DA neurons (26,27) and linked to the degeneration of A9 DA neurons in the *weaver* mouse (26,41,42). We tested whether an increase in GIRK2 expression levels could modulate vulnerability to MPP^+ in PC12-αSyn. Lentivirus-mediated overexpression of GIRK2 in PC12-αSyn (Fig. 3A and 3B) resulted in significantly increased vulnerability at low (1 mM) and high (5 mM) concentrations of MPP^+ when compared with control (eGFP-transduced) cells (Fig. 3C). Then, we characterized GIRK2 expression in TH-positive cells of primary VM cultures (Fig. 3D and 3E). These cultures contained a mixed cell population of A9- and A10-like DA neurons and ∼40% of the TH-positive neurons at 5 days *in vitro* were GIRK2-positive by immunocytochemistry (Fig. 3E). The number of TH-positive/GIRK2-positive cells was reduced following MPP^+ treatment, presumably reflecting vulnerability to this mitochondrial toxin when compared

Table 1. The differentially expressed genes between A9 and A10 DA neurons (>2-fold, FDR < 1%)

Fold change	UniGene name	Mean signal (A9)	Mean signal (A10)	Symbol	*P*-value	mRNA accession no.
More expressed in A9 DA neurons						
6.4	Aldehyde dehydrogenase family 1, subfamily A7	5912	853	Aldh1a7	6.55E − 14	NM_011921
5.3	Thyrotropin releasing hormone receptor	1984	329	Trhr	4.77E − 14	M59811
4.3	CD24a antigen	1870	350	Cd24a	5.24E − 07	BB560574
4.3	CD24a antigen	2585	565	Cd24a	4.73E − 14	NM_009846
3.7	Fibroblast growth factor 1	7293	1833	Fgf1	4.73E − 14	AI649186
3.4	Nuclear receptor interacting protein 3	18532	5524	Nrip3	4.73E − 14	NM_020610
3.4	Membrane protein, palmitoylated 6 (MAGUK p55 subfamily member 6)	2384	611	Mpp6	4.99E − 14	AF199010
3.1	RAB3C, member RAS oncogene family	2397	712	Rab3c	4.77E − 14	AY026947
3.1	Glutamate receptor, ionotropic, NMDA2C (epsilon 3)	2797	783	Grin2c	4.77E − 14	NM_010350
3.0	Poliovirus receptor-related 3	1457	426	Pvrl3	4.73E − 14	NM_021495
2.9	Solute carrier family 25 (mitochondrial carrier, adenine nucleotide translocator), member 5	4248	1458	Slc25a5	3.70E − 06	AV003169
2.9	SRY-box containing gene 6	1877	581	Sox6	4.73E − 14	AJ010605
2.8	Cerebellin 1 precursor protein	4532	1580	Cbln1	2.35E − 13	AA016422
2.8	Secreted phosphoprotein 1	531	157	Spp1	4.73E − 14	NM_009263
2.7	Nuclear receptor interacting protein 3	4723	1652	Nrip3	4.73E − 14	NM_020610
2.7	Fibroblast growth factor inducible 15	1327	457	Fin15	1.77E − 11	NM_008016
2.7	Zinc finger, DHHC domain containing 2	1268	436	Zdhhc2	4.73E − 14	BB224658
2.6	Gap junction membrane channel protein alpha 1	1337	464	Gja1	4.73E − 14	M63801
2.6	Solute carrier family 25 (mitochondrial carrier, adenine nucleotide translocator), member 5	1910	710	Slc25a5	7.79E − 07	AV110784
2.6	Galactose mutarotase	683	228	Galm	4.77E − 14	AV307219
2.6	Cytochrome P450, family 4, subfamily v, polypeptide 3	2107	761	Cyp4v3	4.73E − 14	NM_133969
2.6	Vav 3 oncogene	1269	443	Vav3	4.77E − 14	BC027242
2.5	Gap junction membrane channel protein alpha 1	2060	782	Gja1	4.73E − 14	BB142324
2.5	Gap junction membrane channel protein alpha 1	8695	3335	Gja1	4.73E − 14	BB039269
2.5	Solute carrier family 6 (neurotransmitter transporter, GABA), member 1	4143	1603	Slc6a1	3.81E − 09	M92378
2.4	Special AT-rich sequence binding protein 1	5666	2301	Satb1	4.73E − 14	BG092481
2.4	Calneuron 1	4697	1930	Caln1	4.77E − 14	AF282251
2.3	Transcribed sequence with weak similarity to protein ref:NP_055276.1 (H.sapiens) contactin 6; neural adhesion molecule [Homo sapiens]	1589	637	NA	2.95E − 12	AW553181
2.3	Solute carrier family 25 (mitochondrial carrier, adenine nucleotide translocator), member 5	12594	5705	Slc25a5	0.0015354	AV026569
2.3	Neurofilament 3, medium	3018	1272	Nef3	1.02E − 07	NM_008691
2.3	Tyrosinase-related protein 1	1202	498	Tyrp1	4.73E − 14	BB762957
2.2	RAS protein-specific guanine nucleotide-releasing factor 1	1680	698	Rasgrf1	4.73E − 14	NM_011245
2.2	Cerebellin 1 precursor protein	7630	3372	Cbln1	4.73E − 14	AA016422
2.2	Calcium channel, voltage dependent, alpha2/delta subunit 3	8141	3593	Cacna2d3	4.73E − 14	NM_009785
2.2	Solute carrier family 25 (mitochondrial carrier, adenine nucleotide translocator), member 5	15184	7322	Slc25a5	0.00605729	BM210336
2.2	Insulin-like growth factor 1	4068	1766	Igf1	4.73E − 14	BG075165
2.1	Glutamic acid decarboxylase 1	3260	1457	Gad1	1.22E − 10	AF326547
2.1	ATPase, Ca++ transporting, ubiquitous	3612	1528	Atp2a3	8.50E − 10	NM_016745
2.1	Synuclein, gamma	13275	6163	Sncg	1.84E − 07	NM_011430
2.1	Fibroblast growth factor receptor 3	2566	1162	Fgfr3	4.73E − 14	NM_008010
2.1	Protein phosphatase 2, regulatory subunit B (B56), gamma isoform	2376	1128	Ppp2r5c	0.00013414	BC003979
2.1	Protein tyrosine phosphatase, receptor type Z, polypeptide 1	4449	2037	Ptprz1	4.73E − 14	BC002298
2.1	Sorcin	2221	1029	Sri	8.40E − 14	AK008404
2.0	RAS-like, estrogen-regulated, growth-inhibitor	628	289	Rerg	2.38E − 08	BC026463
2.0	ATPase, Na+/K+ transporting, alpha 2 polypeptide	2677	1261	Atp1a2	1.71E − 11	AI845177
2.0	Limb expression 1 homolog (chicken)	2232	1035	Lix1	4.73E − 14	NM_025681
2.0	Aquaporin 4	1295	594	Aqp4	1.99E − 07	BB193413
2.0	Lactate dehydrogenase 2, B chain	40152	20223	Ldh2	1.03E − 05	NM_008492

Continued

Table 1. *Continued*

Fold change	UniGene name	Mean signal (A9)	Mean signal (A10)	Symbol	*P*-value	mRNA accession no.
2.0	Oxysterol binding protein-like 11	1396	660	Osbpl11	3.16E − 07	BM220135
2.0	Deleted in bladder cancer chromosome region candidate 1 (human)	2586	1251	Dbccr1	4.73E − 14	AB060589
2.0	RIKEN cDNA 6230410L23 gene	4137	2041	6230410L23Rik	4.73E − 14	AF282980
2.0	Special AT-rich sequence binding protein 1	4602	2271	Satb1	4.73E − 14	AV172776
2.0	Fibroblast growth factor inducible 15	520	226	Fin15	1.54E − 05	BB388301
2.0	SH3-binding kinase	3095	1493	Sbk	4.73E − 14	BC025837
2.0	RIKEN cDNA 1110039C07 gene	1589	749	1110039C07Rik	3.94E − 07	BC028307
2.0	Acetyl-Coenzyme A dehydrogenase, long-chain	1041	496	Acadl	2.20E − 06	BB728073
2.0	Annexin A1	6547	3253	Anxa1	7.95E − 05	NM_010730
2.0	Solute carrier family 25 (mitochondrial carrier, adenine nucleotide translocator), member 5	12370	6475	Slc25a5	0.00184671	U27316
2.0	Inhibitor of DNA binding 2	487	233	Idb2	4.46E − 06	BF019883
2.0	RIKEN cDNA 1500001H12 gene	1632	772	1500001H12Rik	4.73E − 14	NM_021316
More expressed in A10 DA neurons						
−17.5	Lipoprotein lipase	401	9257	Lpl	7.74E − 14	BC003305
−14.0	Gastrin releasing peptide	652	10045	Grp	6.55E − 14	BC024515
−6.4	Orthodenticle homolog 2 (Drosophila)	282	2176	Otx2	5.51E − 14	BC017609
−5.3	Calcitonin/calcitonin-related polypeptide, alpha	152	990	Calca	4.73E − 14	AF330212
−5.1	Cocaine and amphetamine regulated transcript	570	3423	Cart	4.99E − 14	NM_013732
−5.1	Insulin-like growth factor binding protein 4	891	4981	Igfbp4	5.14E − 14	BB787243
−4.8	Insulin-like growth factor binding protein 4	322	1937	Igfbp4	4.99E − 14	BC019836
−4.6	Colony stimulating factor 2 receptor, beta 2, low-affinity (granulocyte-macrophage)	340	1862	Csf2rb2	4.77E − 14	NM_007781
−4.5	Neurogenic differentiation 6	131	712	Neurod6	8.52E − 12	NM_009717
−4.3	Neuropilin 2	1474	6821	Nrp2	4.99E − 14	BQ176723
−4.3	Adenylate cyclase 7	1112	5476	Adcy7	4.99E − 14	BB746807
−4.2	RIKEN cDNA 0610007P22 gene	1256	5760	0610007P22Rik	6.52E − 14	BC022659
−4.1	Early growth response 1	2017	8102	Egr1	1.19E − 10	NM_007913
−3.9	Growth hormone receptor	6562	25607	Ghr	4.77E − 14	NM_010284
−3.5	Tachykinin receptor 3	2453	9133	Tacr3	2.38E − 09	AV328460
−3.5	Calbindin-28K	164	678	Calb1	4.73E − 14	BB246032
−3.5	Vasoactive intestinal polypeptide	361	1510	Vip	3.90E − 05	AK018599
−3.4	Potassium voltage-gated channel, shaker-related subfamily, member 5	132	538	Kcna5	4.73E − 14	NM_008419
−3.4	FBJ osteosarcoma oncogene	1263	4694	Fos	4.73E − 14	AV026617
−3.3	RIKEN cDNA 2610042L04 gene	4210	14413	2610042L04Rik	4.96E − 14	BM195235
−3.3	RIKEN cDNA 2610042L04 gene	8396	28600	2610042L04Rik	4.83E − 14	BM195235
−3.2	G substrate	491	1874	Gsbs	4.73E − 14	BC026822
−3.2	Reticulocalbin	720	2703	Rcn	4.77E − 14	NM_009037
−3.0	Potassium voltage-gated channel, shaker-related subfamily, beta member 1	982	3643	Kcnab1	1.37E − 10	AF033003
−3.0	FXYD domain-containing ion transport regulator 6	667	2414	Fxyd6	4.73E − 14	AB032010
−3.0	Major urinary protein 1	349	1235	Mup1	4.99E − 14	NM_031188
−3.0	Calbindin-28K	11186	34116	Calb1	4.73E − 14	BB246032
−2.8	Procollagen, type XI, alpha 1	1207	3810	Col11a1	1.15E − 06	NM_007729
−2.8	Double C2, alpha	1013	3117	Doc2a	4.73E − 14	BB543070
−2.8	Neuropilin	896	2734	Nrp	1.87E − 13	AK011144
−2.8	EGL nine homolog 3 (C. elegans)	1765	5114	Egln3	4.77E − 14	BC022961
−2.7	MARCKS-like protein	1728	4940	Mlp	4.73E − 14	AV110584
−2.7	Adenylate cyclase activating polypeptide 1	1239	3623	Adcyap1	4.73E − 14	AI323434
−2.7	Immunoglobulin superfamily, member 4A	861	2485	Igsf4a	2.20E − 13	NM_018770
−2.7	Activated leukocyte cell adhesion molecule	1992	5471	Alcam	4.77E − 14	U95030
−2.7	Solute carrier family 17 (sodium-dependent inorganic phosphate cotransporter), member 6	811	2349	Slc17a6	8.22E − 13	BQ180367
−2.6	DNA sequence AF424697	2844	7832	AF424697	4.73E − 14	AF424697
−2.6	Immunoglobulin superfamily, member 4A	4184	11405	Igsf4a	4.73E − 14	NM_018770
−2.6	Membrane protein, palmitoylated 3 (MAGUK p55 subfamily member 3)	2972	8015	Mpp3	1.02E − 12	NM_007863
−2.6	Cadherin 2	2461	6485	Cdh2	5.14E − 14	BC022107
−2.5	Pleiomorphic adenoma gene-like 1	2472	6302	Plagl1	5.61E − 14	AF147785
−2.5	Calbindin 2	6139	15618	Calb2	4.77E − 14	BC017646
−2.5	B-cell CLL/lymphoma 11A (zinc finger protein)	1444	3746	Bcl11a	1.53E − 09	NM_016707

Continued

Table 1. *Continued*

Fold change	UniGene name	Mean signal (A9)	Mean signal (A10)	Symbol	*P*-value	mRNA accession no.
−2.5	MARCKS-like protein	602	1594	Mlp	4.73E − 14	BB491008
−2.5	Heparan sulfate 6-O-sulfotransferase 2	1244	3263	Hs6st2	1.77E − 11	AW536432
−2.4	CD44 antigen	295	835	Cd44	6.26E − 07	M27130
−2.4	Plexin C1	1756	4493	Plxnc1	4.73E − 14	BB476707
−2.4	Zinc finger protein 179	1058	2727	Zfp179	6.91E − 13	BB546771
−2.4	Erythroid differentiation regulator 1	4205	9987	Erdr1	0.00478427	AJ007909
−2.4	Core binding factor beta	1353	3385	Cbfb	5.61E − 06	NM_022309
−2.3	MARCKS-like protein	751	1841	Mlp	4.73E − 14	AV215438
−2.2	Cholecystokinin	4551	10405	Cck	1.13E − 06	NM_031161
−2.2	Immunoglobulin superfamily, member 4A	3965	8934	Igsf4a	4.73E − 14	NM_018770
−2.2	Odd Oz/ten-m homolog 1 (Drosophila)	3623	8159	Odz1	4.73E − 14	NM_011855
−2.2	Hypothetical protein, MNCb-2622	742	1702	AB041544	5.60E − 09	NM_021416
−2.2	Protocadherin 21	731	1707	Pcdh21	1.12E − 07	NM_130878
−2.1	Sortilin-related VPS10 domain containing receptor 3	980	2259	Sorcs3	4.73E − 14	AK018111
−2.1	Cysteine-rich motor neuron 1	1157	2475	Crim1	5.14E − 05	AK018666
−2.1	Pleckstrin homology-like domain, family A, member 1	1212	2713	Phlda1	3.04E − 13	NM_009344
−2.1	Single-stranded DNA binding protein 3	2956	6422	Ssbp3	4.73E − 14	AV295012
−2.1	Myosin, heavy polypeptide 7, cardiac muscle, beta	452	1062	Myh7	3.87E − 08	NM_080728
−2.1	RIKEN cDNA 0610011I04 gene	450	1015	0610011I04Rik	4.73E − 14	BC006049
−2.1	Procollagen, type IV, alpha 1	1593	3443	Col4a1	4.73E − 14	BF158638
−2.1	Neuropilin	498	1122	Nrp	8.14E − 12	AK011144
−2.0	Gastrokine 1	275	625	Gkn1	9.73E − 13	AV081751
−2.0	Ribosomal protein S27	4497	9679	Rps27	2.53E − 06	AA208652
−2.0	Amylase 1, salivary	2990	6237	Amy1	4.73E − 14	NM_007446
−2.0	Ryanodine receptor 2, cardiac	755	1673	Ryr2	4.08E − 06	NM_023868
−2.0	FK506 binding protein 9	1002	2127	Fkbp9	6.89E − 10	BB026630
−2.0	RIKEN cDNA 2410012A13 gene	605	1323	2410012A13Rik	4.73E − 14	NM_023396
−2.0	Histocompatibility 2, Q region locus 1	75	156	H2-Q1	1.03E − 08	U96752
−2.0	G protein-coupled receptor 83	893	1856	Gpr83	5.27E − 07	BB110067
−2.0	RIKEN cDNA 2410018L13 gene	7895	15701	2410018L13Rik	2.78E − 10	NM_016677
−2.0	Ribonuclease L (2′, 5′-oligoisoadenylate synthetase-dependent)	484	1008	Rnasel	4.73E − 14	BF714880

Table 2. Validation of microarray results by real-time PCR on RNA samples collected by LCM

	Category	Accession no.	Gene	Gene symbol	Fold change	*P*-value
A9	Growth factor	AI649186	Fibroblast growth factor 1	Fgf1	4.7 ± 0.4	0.0046
		BG075165	Insulin-like growth factor 1	Igf1	2.5 ± 0.1	0.0003
		NM_008010	Fibroblast growth factor receptor 3	Fgfr3	3.7 ± 0.9	0.0490
	Mitochondrial protein	AV003169	Adenine nucleotide translocase 2	Slc25a5	2.4 ± 0.4	0.0325
	Energy metabolism	NM_008492	Lactate dehydrogenase 2, B chain	Ldh2	2.6 ± 0.5	0.0407
	Vesicle-mediated transport	AY026947	RAB3C	Rab3c	5.0 ± 0.6	0.0154
		AV339290	RAB14	Rab14	2.2 ± 0.2	0.0049
	Enzyme-linked receptor/phosphatase	BC002298	Protein tyrosine phosphatase z-polypeptide 1	Ppp2r5c	2.3 ± 0.4	0.0425
	Apoptosis	NM_007611	Caspase 7	Casp7	2.6 ± 0.4	0.0472
	Cell surface molecules	BB560574	CD24a	Cd24a	5.6 ± 0.9	0.0193
A10	Neuropeptide	NM_013732	Cocaine and amphetamine regulated transcript	Cart	4.7 ± 0.3	0.0037
		AI323434	Pituitary adnylate cyclase activating polypeptide	Adcyap1	3.1 ± 0.6	0.0428
		AK018599	Vasoactive intestinal polypeptide	Vip	4.4 ± 1.0	0.0453
		BC024515	Gastrin releasing peptide	Grp	8.5 ± 2.0	0.0318
	Calcium binding protein	NM_009037	Reticulocalbin	Rcn	4.3 ± 0.1	0.0037
		BB246032	Calbindin D28K	Calb1	2.9 ± 0.6	0.0300

Fold changes are presented as average ± SEM with *P*-values (one sample *t*-test).

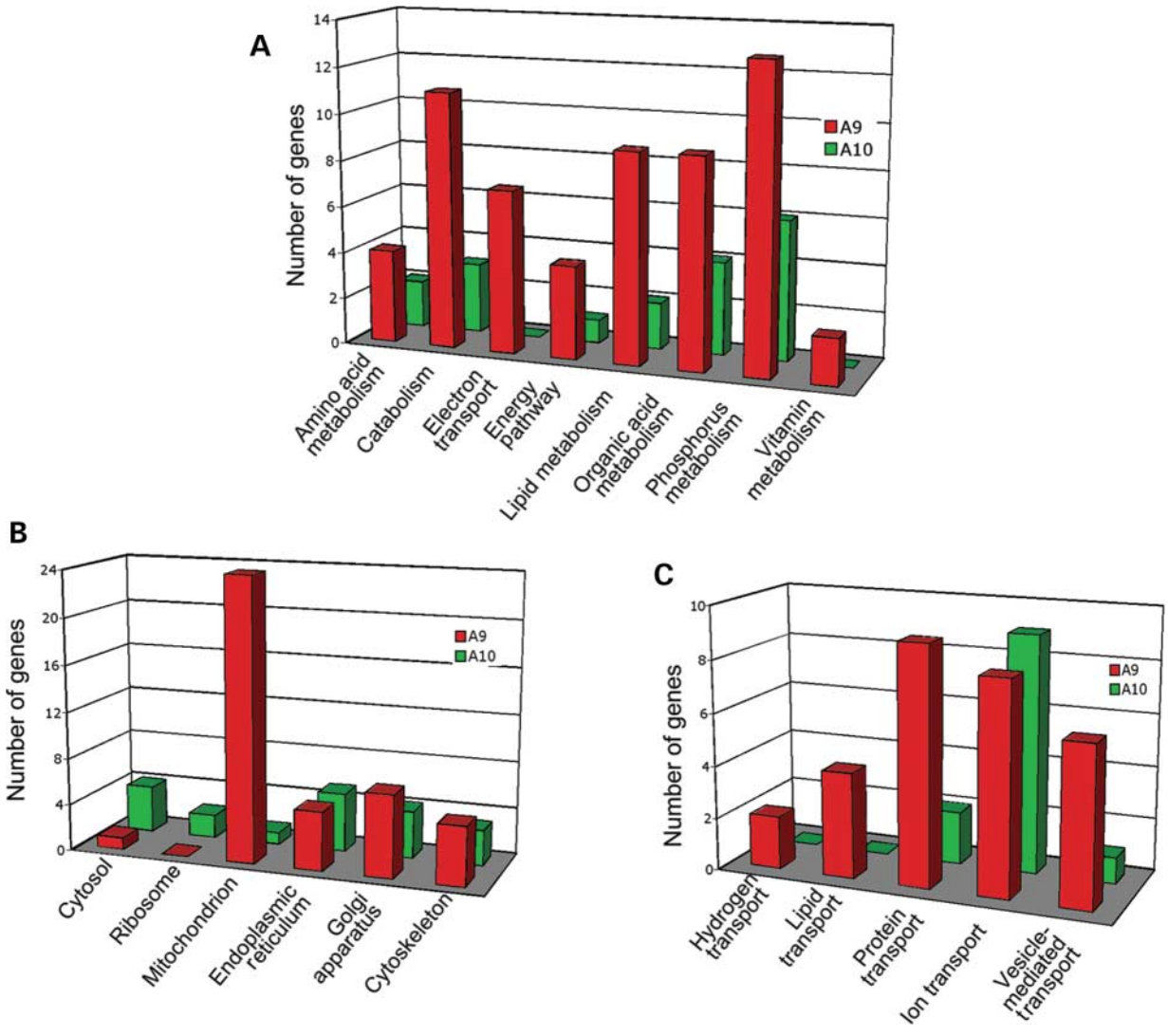

Figure 2. Functional profiles of microarray data. A9- and A10-elevated genes were categorized based on biological functions and cellular components by Onto-Express (36). Genes with significant differences (FDR < 1%) were distributed into different categories of metabolisms (**A**), cellular components in cytoplasm (**B**) and transport mechanisms (**C**).

with TH-positive/GIRK2-negative cells (Fig. 3E). We also examined a role of a mitochondrial protein, adenine nucleotide translocase (ANT) 2, which was elevated in A9 neurons (Table 2) on MPP^+ induced toxicity. ANTs appear to have an essential role in regulating permeability transition of mitochondria (43), which may in turn induce apoptosis (44). As ANT-2 mRNA was abundant in PC12 cells (data not shown), we inhibited the activity of ANT-2 by applying its inhibitor, bongkrekic acid (BA) in the presence of MPP^+. BA was able to decrease MPP^+-induced LDH release in a dose-dependent manner (Fig. 3F), indicating that higher expression of ANT-2 may increase susceptibility to MPP^+ toxicity. In primary VM cultures, BA showed a significant protective effect on both GIRK2-negative and GIRK2-positive DA neurons (Fig. 3G). Interestingly, GIRK2-negative DA neurons appeared to be more sensitive to BA, as these A10-like DA neurons were maximally protected at lower doses than GIRK2-positive DA neurons (Fig. 3G).

On the basis of our comparative genetic profiles (Table 3), many growth factor-related genes were differentially expressed. Among these, we analyzed IGF-1 in both PC12-αSyn cells and primary VM cultures. IGF-1 was able to exert protective effects against MPP^+ toxicity in both PC12-αSyn cells (Fig. 3H) and GIRK2-positive DA neurons of primary VM culture (Fig. 3I) in a dose-dependent manner.

Altered vulnerability of α-synuclein overexpressing PC12 cells and primary VM cultures by molecules elevated in A10 DA neurons

We also analyzed molecules that were more highly expressed in A10 DA neurons. Neuropeptides were chosen for analysis

Table 3. Comparison of genetic profiles in A9 and A10 DA neurons from microarray analyses (>1.5-fold, FDR < 1%)

	A9	A10
Neuropeptide/hormone related	Secreted phosphoprotein 1	Cocaine and amphetamine regulated transcript
	Neuropeptide Y receptor Y5	Calcitonin/calcitonin-related polypeptide, alpha
	Neurotensin receptor 2	Colony stimulating factor 2 receptor, beta 2
	Colony stimulating factor 1 receptor	Growth hormone receptor
	Inhibin beta-B	Gastrin releasing peptide
		Vasoactive intestinal polypeptide
		Tachykinin receptor 3
		Pituitary adenylate cyclase activating polypeptide
		Gastrokine 1
		Cholecystokinin
		Cholecystokinin A receptor
		Arginine vasopressin receptor 1A
Growth factor related	Fibroblast growth factor 1	
	Fibroblast growth factor receptor 3	
	Fibroblast growth factor inducible 15	
	Insulin-like growth factor 1	
	Epidermal growth factor pathway substrate 8	
Axon guidance related	Eph receptor A7	Neuropilin 1
		Neuropilin 2
		Ephrin B2
		Ephrin B3
		Plexin C1
		Slit 2
Proteases	Caspase 7	
	Protease, serine,11 (Igf binding)	
Protease inhibitors		Plexin C1
		Cysteine-rich motor neuron 1
		Serine protease inhibitor, Kunitz type2
Phosphatases	Protein tyrosine phosphatase z polypeptide 1	
	Protein tyrosine phosphatase, non-receptor type 5	
	Protein phosphatase 2, regulatory subunit B (B56) alpha isoform	
	Protein phosphatase 2, regulatory subunit B (B56) gamma isoform	
Phosphatase inhibitor		G-substrate
Apoptosis	Caspase 7	Pleomorphic adenoma gene-like 1
	Bcl-2 like 11 (apoptosis facilitator, Bim)	Mitogen activated protein kinase kinase kinase 5
	Mitogen activated protein kinase 9	
	Estrogen-related receptor β like 1	
	Programmed cell death 10	

because they were a prominent class of molecules expressed relatively higher in A10 DA neurons (Tables 2 and 3). Gastrin releasing peptide (GRP), calcitonin/calcitonin gene-related peptide alpha (CGRP) and pituitary adenylate cyclase activating polypeptide (PACAP) were individually applied in the presence of MPP^+ in PC12-αSyn cells or primary VM cultures. GRP exhibited a dose-dependent neuroprotective effect on both PC12-αSyn cells and GIRK2-positive DA neurons of primary VM cultures (Fig. 4A and 4B). CGRP was also able to significantly reduce MPP^+-induced LDH release in PC12-αSyn cells (Fig. 4C). In primary VM culture, it had no effect on GIRK2-positive DA neurons, whereas it exhibited a significant toxic effect on GIRK2-negative DA neurons at higher doses (Fig. 4D). PACAP was able to reduce MPP^+ toxicity in PC12-αSyn cells and in GIRK2-positive and GIRK2-negative DA neurons of primary VM cultures in a dose-dependent manner (Fig. 4F and 4E). These results support the hypothesis that certain molecules with differential expression patterns between A9 and A10 DA neurons may play key roles in protection and vulnerability of DA neurons.

DISCUSSION

In this study, we used LCM and genomic profiling to characterize the innate physiological differences between A9 and A10 DA midbrain neurons. Despite an overall high similarity in the gene expression profiles of these related DA neurons, several genes from different biological categories showed cell type-specific expression patterns. We examined some of these differentially expressed molecules using PC12-αSyn cells and

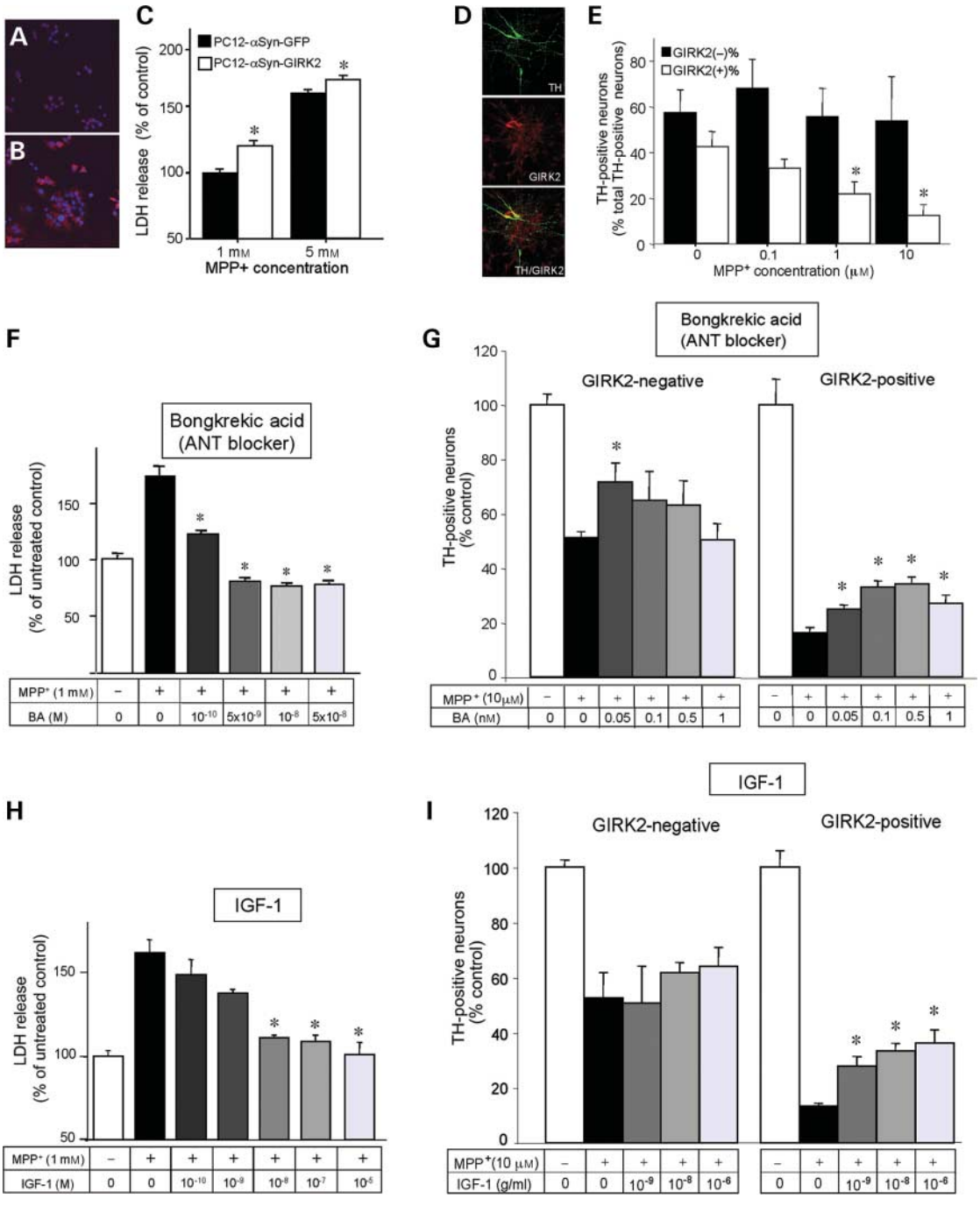

Figure 3. Altered vulnerability of PC12-αSyn cells and primary VM cultures by A9-elevated molecules. (**A–C**) Effects of GIRK2 overexpression in PC12-αSyn cells. Cells were transduced with either eGFP or GIRK2-expressing lentiviruses at an MOI of 5 and higher GIRK2 expression was achieved in GIRK2-transduced cells (B) when compared with untransduced cells (A). Red staining represents GIRK2 and cell nuclei were visualized by DAPI staining (blue). There was higher MPP^+ toxicity in GIRK2 overexpressing PC12-αSyn cells (1 and 5 mM) when compared with eGFP-expressing control cells (C). Cell viability was measured by LDH release, which was significantly increased in GIRK2 overexpressing cells when compared with control eGFP-expressing cells ($^*P < 0.05$ between groups). (**D–E**) Differential vulnerability of primary VM cells to MPP^+. (D) Immunostaining of primary VM cultures demonstrated TH(+), GIRK2(+) and TH(+)/GIRK2(+) cells. (E) TH(+)/GIRK2(+) or TH(+)/GIRK2(−) cells were counted after MPP^+ treatment and were presented as percentage of total TH(+) neurons of non-treated control conditions. TH(+)/GIRK2(+) cells were more vulnerable to MPP^+ than TH(+)/GIRK2(−) cells [$^*P < 0.05$ in comparison with the control (no MPP^+) condition]. (**F–I**) The effects of an ANT blocker, BA and IGF-1 in PC12 αSyn cells (F and H) and in primary VM cultures (G and I). In PC12 αSyn cells (F and H), cells were pretreated with BA (F) and IGF-1 (H) at concentrations indicated under the bar graph for 2 h prior to treatment with 1 mM MPP^+ for 24 h. The levels of LDH release were presented as percentage of control group without treatment. LDH releases were significantly reduced by addition of these protective molecules [$^*P < 0.01$ in comparison with the group of MPP^+ only treatment (black bar graph); Student's *t*-test]. In primary VM cultures (G and I), the ANT blocker (G) and IGF-1 (I) were added to the cultures at 5 days *in vitro* 2 h prior treatment with 10 μM MPP^+. After 48 h, TH(+)/GIRK2(+) and TH(+)/GIRK2(−) neurons were counted and presented as percentage of total TH(+) neurons of control (no MPP^+) conditions [$^*P < 0.05$ in the comparison with the group of MPP^+ only treatment (black bar graph)]. Student's *t*-test was used to obtain statistical significance.

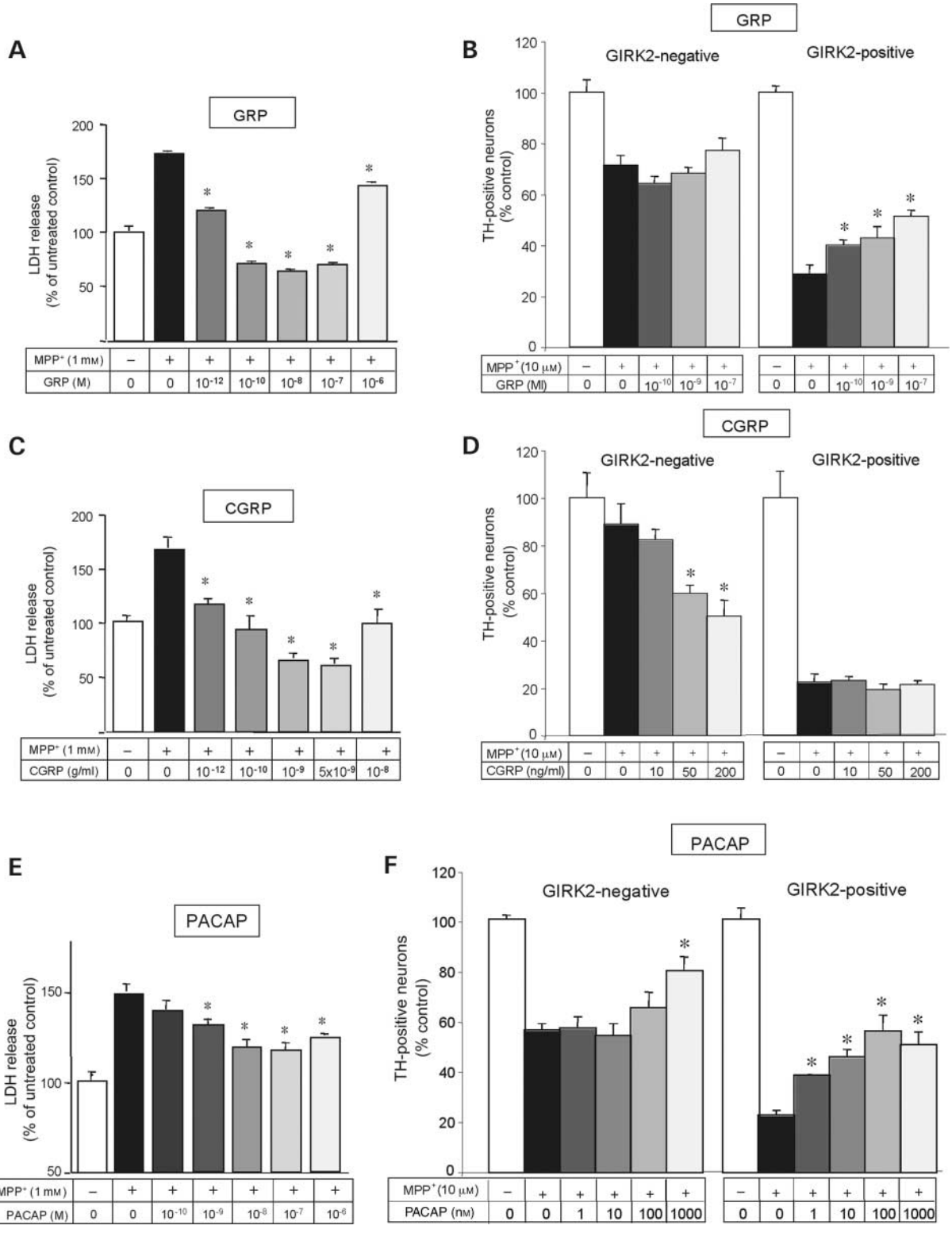

Figure 4. Altered vulnerability of PC12-αSyn cells and primary VM cultures by A10-elevated molecules. In PC12 cells (**A**, **C** and **E**), cells were pretreated with GRP (A), CGRP (C) and PACAP (E) with concentrations indicated under the bar graph for 2 h prior to 1 mM MPP^+ treatment for 24 h. The levels of LDH release were presented as percentage of control group without treatment. Significant dose-dependent decreases in LDH release were detected in these experiments indicating neuroprotective effects of these peptides from toxic insult [$^*P < 0.01$ in the comparison with the group of MPP^+ only treatment (black bar graph); Student's *t*-test]. In primary VM cultures (**B**, **D** and **F**), GRP (B), CGRP (D) and PACAP (E) were added to the cells at 5 days *in vitro* 2 h prior to treatment with 10 μM MPP^+. After 48 h, TH(+)/GIRK2(+) and TH(+)/GIRK2(−) neurons were counted and presented as percentage of total TH(+) neurons of control (no MPP^+) conditions [$^*P < 0.05$ in the comparison with the group of MPP^+ only treatment (black bar graph)]. Student's *t*-test was used to obtain statistical significance.

primary VM cultures exposed to the PD-related neurotoxin, MPP^+. Results from these bioassays showed that neuropeptides (GRP, CGRP and PACAP) expressed predominantly in A10 DA neurons protected against MPP^+. Of genes elevated in A9 DA neurons, growth factors such as IGF-1 also decreased the vulnerability, whereas ANT-2 and GIRK2 appeared to increase cell toxicity. These results suggest that the study of genes with differential expression levels between A9 and A10 midbrain DA neurons can provide insights into specific neuroprotective and/or degenerative responses.

We propose at least two possible mechanisms whereby differential gene expression in A9 DA neurons could alter the vulnerability to neurotoxins. First, certain molecules may by themselves confer increased susceptibility in these neurons when their expression levels are relatively elevated. Elevated expression of such molecules may then decrease the threshold to extrinsic and intrinsic factors leading to cell-type specific degeneration (31,32). For example, GIRK2 and ANT-2 may render A9 DA neurons more vulnerable because of their pathophysiological actions on the membrane potential and on the mitochondrial permeability transition, respectively (discussed subsequently). Or pro-apoptotic molecules, such as caspase 7 and Bim (38) in A9 DA neurons (Table 3), may increase susceptibility of these neurons in pathological conditions. A second possibility is that A9 DA neurons may be more functionally dependent upon molecules with higher expression and therefore more vulnerable to fluctuation in their levels. In such cases, any insult, genetic polymorphisms or an age-dependent decrease in expression levels (45) that reduces the physiological functions of these molecules may be neurotoxic. An example of this class of A9-elevated molecule might be IGF-1, a known neuroprotective factor (46,47).

GIRK controls the neuronal membrane excitability by selectively permitting the flux of K^+ ions near the resting membrane potential (48). Among four isoforms of GIRK, only GIRK2 is exclusively expressed in vulnerable DA neurons (26,27). GIRK2 generates a slow IPSP in DA neurons via activation of D_2 or $GABA_B$ receptors and controls the membrane excitability of DA neurons. A potential role of GIRK2 in A9 DA neuron pathology in PD has been revealed in *weaver* mice, which have a spontaneous mutation in the GIRK2 gene and display PD-like patterns of DA neuron degeneration (28–30). Mutation in GIRK2 decreases the channel selectivity for K^+, leading to the destabilization of the cell membrane (49). Our data suggest that elevated expression levels of GIRK2 may also contribute to the increased vulnerability of A9 DA neurons.

ANT is thought to play a role in the transport of ADP and ATP across the mitochondrial inner membrane (43,50). In addition, it is involved in the formation of the mitochondrial permeability transition pore (mPTP), a non-specific pore that is an important mediator of apoptosis (43,50). The mPTP opens in response to stimuli including reactive oxygen species and inhibitors of the electron transport chain, including MPP^+ (51). In our study, blocking the function of ANT-2 by BA decreased the vulnerability of both PC12-αSyn cells and primary VM culture neurons to MPP^+. This demonstrates that inhibition of ANT-2 is neuroprotective and, therefore, elevated ANT-2 expression levels in A9 DA neurons could confer increased susceptibility of these neurons to oxidative stress and toxins such as MPP^+. It is interesting to note the toxic effect of BA at higher doses (Fig. 3G). It is unlikely that the toxic effect is due to non-specific inhibition of other proteins by BA as the doses used in our experiments are much lower than what is conventionally used in the field (44,52). However, it could be that the unusual dose–response curve of BA may depend on ANT's dual functions. Under pathological conditions, ANT is involved in forming the mPTP, which leads to cell death (44,50). Thus, blocking the mPTP-forming function of ANT would be protective to cells. However, under physiological conditions, ANT imports ADP from the cytosol and exports ATP synthesized by mitochondria back to the cytosol to be used as an energy source. Therefore, inhibition of ANT's physiological function could then be toxic (52). At the MPP^+ concentration used in our experiment, some ANT molecules may be involved in mPTP formation, but the remainder may still function as ADP/ATP carriers. At higher doses, this normal physiological function of ANT could be inhibited, thus depleting the cellular energy source and deleteriously affecting cell survival.

IGF-1 is neuroprotective in brain hypoxia–ischemia (53,54), axotomy (55), age-induced hippocampal death (56) and glutamate-induced motor neuron death (57). It protects embryonic DA neurons from apoptosis (58) and dopaminergic cells from toxin-induced cell death *in vitro* (59). In addition, IGF-1 or the N-terminal tripeptide of IGF-1 protected DA neurons and improved functional deficits in 6-OHDA treated rats (46,47). Consistent with these findings, application of IGF-1 to the medium also reduced the MPP^+ toxicity in PC12-αSyn cells and A9-like DA neurons of primary VM cultures in our study. This supports the notion that IGF-1 is an important neuroprotective factor which A9 DA neurons may depend on. Interestingly, plasma IGF-1 levels decrease with age (60) and a causal relationship between age-dependent decrease in IGF-1 and reduced cognitive brain function has been proposed in many studies (61). Taken together, the reduction of IGF-1 due to aging may contribute to increased vulnerability of A9 DA neurons in PD.

In our study, A10 DA neurons showed elevated transcription levels of several neuropeptides. We selected GRP, CGRP and PACAP to examine their roles in protecting DA cells from MPP^+-induced toxicity. GRP is a neuroendocrine peptide known to act primarily in the enteric and central nervous systems, where it regulates diverse functions, from satiety and smooth muscle contraction to the release of other gastrointestinal hormones (62). It has also been studied extensively in the context of cancer cells where it plays a role as an autocrine growth factor (63,64). Although the presence of GRP in SN was reported many years ago (65), its function in DA neurons has not been described. In this study, our microarray data raised the possibility that GRP might be protective to DA neurons and we show here for the first time that GRP could reduce the toxic responses of both PC12-αSyn cells and primary mesencephalic DA neurons against MPP^+. We thus suggest that GRP may contribute to the reduced susceptibility of A10 DA neurons in PD.

CGRP exerts multiple biological actions in the central nervous, gastrointestinal and cardiovascular systems (66,67). CGRP also influences the differentiation of immature DA

neurons in primary VM cultures by inducing neurite outgrowth and increasing DA uptake per neuron, but not their normal rate of survival (68). In our study, CGRP reduced mitochondrial toxicity of PC12-αSyn cells. In primary VM cultures, it increased the susceptibility of A10-like DA neurons to the toxin in a dose-dependent manner, whereas it had no effect on the survival of A9-like DA neurons. These data raise the possibility that CGRP may not be a neuroprotective factor for DA neurons. However, it should be noted that primary VM cultures represent not adult but immature neurons. Given that there was a positive effect observed in PC12-αSyn cells, one cannot exclude a potential protective effect of CGRP in adult DA neurons *in vivo.*

PACAP belongs to the family of peptides containing secretin, glucagons and vasoactive intestinal peptide (VIP) (69,70). It is thought to act as a neurotrophic factor during development and as a neuroprotective factor against various insults (71,72). PACAP is also neurotrophic for TH-positive neurons in primary VM culture (73,74). In our *in vitro* assays, PACAP reduced the toxic responses of both the PC12-αSyn cells and the DA neurons of primary VM cultures to MPP^+. In addition, the results from the primary VM cultures demonstrated that A9-like DA neurons were more responsive to the effects of PACAP than A10-like DA neurons. This result is further substantiated by a recent study in which injection of PACAP into the SN protected DA neurons and improved behavioral deficits in a rat model of PD (73). Another neuropeptide from the same class, VIP is also expressed higher in A10 DA neurons (Table 2) and its neurotrophic and neuroprotective effects in DA neurons against MPP^+ have also been reported in a mouse model of PD (75). These data indicate that some A10-elevated molecules may contribute to the reduced vulnerability of A10 DA neurons, suggesting that these factors may be applied to protect A9 DA neurons. Interestingly, several neuropeptides, including PACAP and VIP, are known to be transported through the blood brain barrier via transmembrane diffusion (76), thus increasing their potential to be utilized in therapies for PD.

The microarray analyses also revealed that genes encoding energy-related metabolism and mitochondrial proteins are highly expressed in A9 DA neurons (Supplementary Material, Table S1). This is particularly interesting as mitochondrial dysfunction is thought to contribute to the etiology of PD (77). Elevated expression levels of these genes in A9 DA neurons are consistent with the notion that this neuronal population is highly energy (ATP)-dependent. Given the role of mitochondria in cellular energy metabolism, A9 DA neurons may be particularly susceptible to toxins such as MPP^+ and rotenone (78) and to mutant α-synuclein or parkin which have been reported to cause mitochondrial dysfunction (79–81).

Another group of genes that are elevated in A9 DA neurons are genes related to vesicle-mediated transport, including RAB1, RAB3C, RAB6, RAB11A, RAB14, vacuolar protein sorting 35 and very low density lipoprotein receptor (Supplementary Material, Table S1). Efficient DA sequestration into vesicles protects DA neurons from the deleterious effects of DA oxidation (82). As A9 DA neurons have higher levels of the DA transporter than A10 or hypothalamic (A11, A13–A15) DA neurons (83–86), vesicle-mediated transport may be a more active and critical physiological process in this neuronal population. Interestingly, vesicle-mediated transport genes have recently been recognized as susceptibility factors in PD (45,87,88). In a genome-wide yeast screen for modifiers of α-synuclein-induced toxicity, modifiers were most prominently clustered in the vesicle-mediated transport and lipid metabolism categories (87). Furthermore, several vesicle-mediated transport genes, including several RAB genes, were found within genomic linkage regions for PD (88), and many vesicular transport genes were downregulated after age 40 in a recent study describing aging-dependent changes in human frontal cortex transcriptional profiles (45). This suggests that defective vesicular transport may contribute to the increased susceptibility of the aged patient population to neurodegenerative diseases. Taken together, A9 DA neurons may be particularly vulnerable to genetic or environmental factors that diminish the function of the vesicle-recycling machinery.

A recent paper published after the completion of our study described gene expression differences between catecholaminergic neurons in the rat (89). Although the study was done in rat tissue using a different microarray platform (14 800 element cDNA array), many of the genes the authors reported are consistent with the expression patterns seen in the mouse midbrain DA neuron microarray analysis reported here (Affymetrix oligonucleotide array with 22 000 probes). In addition to the microarray results, our study also includes the quantitative validation by real-time PCR and functional analyses, which illustrate that these differences in phenotypic gene expression may be relevant to neurotoxic responses.

In summary, we used LCM, microarray analysis and real-time PCR to determine gene expression profiles of A9 and A10 midbrain DA neurons and have begun to screen some of the molecules using *in vitro* bioassays. These data may offer opportunities for further *in vivo* modeling of neuroprotective and neurotoxic responses in midbrain DA neurons. Such scientific work may ultimately provide clues to pathogenetic mechanisms involved in PD and delineate neuroprotective and therapeutic interventions against this disease.

MATERIALS AND METHODS

Laser capture microdissection

Tissue preparation. Adult C57/B6 mice (Jackson Laboratory, West Grove, PA, USA) were anesthetized with intraperitoneal (i.p.) sodium pentobarbital (300 mg/kg) and decapitated. The brain was removed, snap-frozen in dry ice-cooled 2-methylbutane (−60°C). Ten micron-thick coronal sections of the midbrain were cut using a cryostat, mounted on LCM slides (Arcturus Engineering, Inc., Mountain View, CA, USA) and immediately stored at −70°C.

Quick immunostaining and dehydration of sections. A quick immunostaining protocol for TH was used to identify the DA neurons to be captured. First, the tissue sections were fixed in cold acetone for 5 min. The slides were then washed in phosphate-buffered saline (PBS), incubated with rabbit anti-TH (Pel-Freez Biologicals, Rogers, AR, USA; 1:25) for 4 min, washed in PBS and exposed to biotinylated

anti-rabbit antibody (Vector Laboratories, Burlingame, CA, USA; 1:25) for 4 min. The slides were washed in PBS, incubated in ABC-horseradish peroxidase enzyme complex (Vectastain, Vector Laboratories) for 4 min and the staining was detected with the substrate, diaminobenzidine (DAB). Sections were subsequently dehydrated in graded ethanol solution (30 s each in water, 70% ethanol, 95% ethanol, 100% ethanol, and twice for 5 min in xylene). On the basis of our qualitative assessment, the sensitivity of the quick TH staining protocol did not differ from regular staining protocols, providing similar intensities of TH staining between A9 and A10 regions.

LCM of mouse midbrain tissue. The PixCell II System (Arcturus Engineering, Inc.) was used for LCM. Five-hundred to seven-hundred neurons were captured in each region of A9 and A10 in each animal. Five replicates of A9 samples were from five different mice and six replicates of A10 samples were from six different mice. As ventrolateral A9 DA neurons are the most vulnerable and medial A10 DA neurons the most resistant to degeneration, only ventrolateral A9 [ventrolateral SNc and SN pars reticulata (SNr)] and medial A10 DA neurons [central linear nucleus (CLi), interfascicular nucleus (IF), medial VTA, medial nucleus paranigralis (PN), medial nucleus parabrachialis pigmentosus (PBN)] were microdissected (Fig. 1A–1D).

Affymetrix GeneChip microarrays

Sample and array processing. Total RNA was separately extracted from the individual replicate samples using the PicoPure RNA isolation kit (Arcturus Engineering, Inc.). Nanogram quantities of total RNA from each sample were used to generate a high fidelity cDNA, which is modified at the 3′ end to contain an initiation site for T7 RNA polymerase. Upon completion of cDNA synthesis, all of the product was used in an *in vitro* transcription (IVT) reaction to generate aRNA. Up to 2 μg of aRNA was used for a second round of amplification which was initiated by random hexamer priming for first strand cDNA synthesis. The second round IVT contained biotinylated UTP and CTP which are utilized for detection following hybridization to the oligonucleotide microarray. Twenty micrograms of full-length cRNA, from both controls and enriched samples, were fragmented and hybridized to GeneChip arrays following the manufacturer's protocol. All samples were subjected to gene expression analysis via the Affymetrix Murine 430A high-density oligonucleotide array, which queries 22 000 mouse probe sets. Protocols for target hybridization, washing and staining were performed according to the manufacturer's protocol (http://www.affymetrix.com).

Data normalization and statistical analysis. Several complementary data analysis approaches were used to identify differentially expressed genes. The Gene Chip Operating System 1.0 (GCOS, Affymetrix) was employed to generate one approach to comparative analysis presented in this study. Distinct algorithms were used to determine the absolute call, which distinguishes the presence or absence of a transcript, the differential change in gene expression and the magnitude of change, which is represented as signal log ratio (on a log base 2 scale). The mathematical definitions for each of these algorithms can be found in the GCOS data analysis guide. Two additional low level analysis methods were applied to all data sets outside of the Affymetrix normalization schema. Iobion's GeneTraffic MULTI was used to perform Robust Multi-Chip Analysis (RMA), which is a median polishing algorithm used in conjunction with both background subtraction and quantile normalization approaches. For each normalization approach, statistical analysis using the Significance Analysis Tool set in GeneTraffic was utilized. A two class unpaired analytical approach employing Benjamini–Hochberg correction for false discovery rate (FDR) was used for all probe level normalized data. Gene lists of differentially expressed genes were generated from this output for functional analysis. All data were organized in a central database in the University of Rochester Functional Genomics Center and are accessible through the following URL (www.fgc.urmc.rochester). Following each of these normalization approaches, all genes differentially expressed were clustered based on biological relevance utilizing both hierarchical and K-means clustering techniques.

Real-time PCR for candidate gene validation

RNA samples from A9 and A10 DA neurons were reverse-transcribed into cDNA using Sensiscript reverse transcriptase (Qiagen, Valencia, CA, USA) and oligo dT as the primer. PCR reactions were set up in 25 μl reaction volume using SYBR Green PCR Master Mix (Applied Biosystems, Foster City, CA, USA). Primers for each candidate gene were designed using MacVacter 7.0 and used with a final concentration of 250 nM. For each primer pairs, duplicates of three to five independently collected A9 and A10 samples were compared to quantify relative gene expression differences between these cells using the $2^{-\Delta\Delta CT}$ method (90). Beta-actin was used as an internal control gene. β-actin was selected not only because it is widely used as a housekeeping gene, but also because it did not show differential expression between A9 and A10 DA neurons based on our microarray analysis. We also compared β-actin with other genes that do not show differential expression based on our microarray analysis, such as capping protein (NM_009798) and alex3 (NM_027870). A9/A10 ratios of these genes, when normalized with β-actin, were approximately 1, which means that all three genes are not differentially expressed between A9 and A10 DA neurons. On the basis of this, we decided to use β-actin as an internal control gene. Primers for candidate genes with approximately equal (within 5% difference) amplification efficiency to that of the internal control were chosen. The *P*-value for real-time PCR results was calculated by one-sample *t*-test.

Generation of GIRK2-expressing lentivirus

Construction of lentiviral vectors. The mouse GIRK2 cDNA (a gift from Dr David Clapham, Children's Hospital, Boston, MA, USA) was cloned into the lentiviral vector, pRRL.cPPT.PGK.GFP.W.Sin-18 vector (kindly provided by Drs R. Zufferey and D. Trono, University of Geneva,

Switzerland) by exchanging the GFP gene with the GIRK2 cDNA and confirmed by sequence analyses.

Production of lentiviral vectors and cell transduction. The lentiviral vector system used in our studies was kindly provided by Drs R. Zufferey and D. Trono, University of Geneva, Switzerland. High titer of infectious lentiviral particles were produced in 293 T-cells using a four-plasmid transfection protocol (*Current Protocols in Neuroscience*, 2000, 4.21.1–4.21.12). For this, the following packaging plasmids pMDLg/pRRE (for *gag* and *pol* expression), pMD.G (for expression of the VSV-G *env* protein) and pRSV.Rev (for *rev* expression) were co-transfected with the recombinant pRRL.cPPT.GIRK2.W.Sin-18 vector to produce viral transduction units (TU). Virus supernatants were collected and filtered through a 0.2 μM filter and either used freshly, stored at −80°C or ultracentrifuged to obtain high concentrations of viral stocks. Virus titers were determined according to published protocols (91) measuring the viral capsid protein p24 by ELISA in collaboration with Dr C. Brander, AIDS Research Center, Massachusetts General Hospital. For *in vitro* transduction, PC12-αSyn were cultured directly in virus-containing media supplemented with 8 μg/ml polybrene.

In vitro functional analysis of candidate molecules

α-Synuclein overexpressing PC-12 cell culture. A PC12 cell line expressing wild-type human α-synuclein was used (kindly provided by Dr Peter Lansbury). α-Synuclein expressing PC12 cells were grown in Dulbecco's modified Eagle's medium (DMEM) (Invitrogen, Carlsbad, CA, USA) supplemented with 10% heat-inactivated horse serum, 5% heat-inactivated fetal calf serum (Hyclone, Logan, UT, USA), 4 mM L-glutamine, streptomycin and penicillin G (Fisher, Pittsburgh, PA, USA). Cells were maintained at 37°C, in 5% CO_2 humid atmosphere. For the bioassay, α-synuclein overexpressing PC-12 cells were treated with 1 mM MPP^+ to determine the neuroprotective effects of BA, insulin growth factor-1 (IGF-1), CGRP alpha, GRP and PACAP molecules. Various doses of the molecules were applied to the cells 2 h prior to MPP^+ treatment and after 24 h, supernatants were collected for measuring a cell-death related release of lactate dehydrogenase (LDH) using an LDH release assay kit (Roche, Indianapolis, IN, USA). BA was purchased from Sigma; IGF-1 from R&D and CGRP, GRP and PACAP from Calbiochem.

Primary VM cell culture. Primary cultures of DA neurons were obtained from E15 Sprague-Dawley rat (Charles River, MA, USA) ventral mesencephalon (VM). The dissected VM tissue was mechanically dissociated with a fine-polished pasteur pipette. The cells were resuspended in DMEM containing heat-inhibited horse serum (10%), glucose (6.0 mg/ml), penicillin, streptomycin and 2 mM glutamine (Gibco). Cell suspensions containing 4×10^5 cells were plated on coverslips in 24-well plates and precoated with a 1:500 diluted solution of polyornithine and fibronectin in 50 mM sodium borate (pH 7.4). For the MPP^+ dose–response curves, cultures were treated at day 5 for 48 h with MPP^+ at concentrations ranging from 0.1 to 10 μM. Neuropeptides, IGF-1 and BA were applied at various doses 2 h prior to 10 μM MPP^+ treatment. After 48 h, cells were fixed in paraformaldehyde for immunostaining of TH and GIRK2.

Immunocytochemistry and stereology

Immunocytochemistry. Indirect immunofluorescence was performed on 4% paraformaldehyde fixed VM cultures. Fixed cells were incubated in a blocking solution consisting of 10% normal donkey serum (Jackson ImmunoResearch Laboratories Inc., West Grove, PA, USA) and 0.1% Triton X-100 (Sigma, St Louis, MO, USA) in 0.1 M PBS for 1 h at room temperature. Primary antibodies were diluted in blocking solution and added to the cells. The primary antibodies used were tyrosine hydroxylase (sheep anti-TH, 1:300, Pel-Freez Biologicals, Rogers, AK, USA) and GIRK2 (rabbit; 1:80, Alomone Laboratories, Jerusalem, Israel). After incubation at 4°C overnight, cells were rinsed three times in 0.1 M PBS for 5 min each before application of the secondary antibody solution for 1 h at room temperature. The secondary antibodies were diluted in 10% normal donkey serum in 0.1 M PBS. Secondary antibodies were Alexa Fluor 488 conjugated donkey anti-sheep and Alexa Fluor 594 conjugated donkey anti-rabbit (Molecular Probes, Eugene, OR, USA). After rinsing in triplicate for 10 min each in 0.1 M PBS, the cells were counterstained with 0.0005% Hoechst 33342 (Molecular Probes) in 0.1 M Tris buffered saline. The coverslips containing the fixed cells were then rinsed in 0.1 M PBS followed by distilled water and mounted onto slides using an aqueous mountant (Gel/Mount, Biomeda Corp., CA, USA). Control coverslips immunostained with secondary antibody only were used to assess specificity of the technique.

Stereology. Design-based stereology was performed by counters blinded to experimental groups on the stained coverslips using an integrated Axioskop 2 microscope (Carl Zeiss, Thornwood, NY, USA) and Stereoinvestigator image capture equipment and software (MicroBrightField, Williston, VT, USA). A contour was drawn around each coverslip to identify the area of interest. A physical dissector probe was utilized and counting frames were placed in a systematically random manner at ∼200 sites/coverslip. The resultant coefficient of error for the stereological counts was used to assess precision ($P < 0.05$).

SUPPLEMENTARY MATERIAL

Supplementary Material is available at HMG Online.

ACKNOWLEDGEMENTS

We thank Dr Vikram Khurana for discussions and reading of the manuscript; Chin-Yi Chu and Oliver Cooper for excellent technical assistance. We also thank Dr Peter Lansbury for providing synuclein overexpressing PC12 cells. This study was conducted in part in the facilities and collaborative

network provided by the Harvard Center for Neurodegeneration and Repair and was supported by funds from the NIH/NINDS P50 Parkinson's Disease Udall Research Centers of Excellence to McLean/Harvard Medical School (PI:OI), USAMRMC grant DAMD 17-01-1-0762 (PI:OI), the Michael Stern Foundation for Parkinson's Disease Research, the Consolidated Anti-Aging Foundation and the Orchard Foundation.

Conflict of Interest statement. None declared.

REFERENCES

1. McRitchie, D.A., Hardman, C.D. and Halliday, G.M. (1996) Cytoarchitectural distribution of calcium binding proteins in midbrain dopaminergic regions of rats and humans. *J. Comp. Neurol.*, **364**, 121–150.
2. Neuhoff, H., Neu, A., Liss, B. and Roeper, J. (2002) I(h) channels contribute to the different functional properties of identified dopaminergic subpopulations in the midbrain. *J. Neurosci.*, **22**, 1290–1302.
3. Wolfart, J., Neuhoff, H., Franz, O. and Roeper, J. (2001) Differential expression of the small-conductance, calcium-activated potassium channel SK3 is critical for pacemaker control in dopaminergic midbrain neurons. *J. Neurosci.*, **21**, 3443–3456.
4. Gorell, J.M., Peterson, E.L., Rybicki, B.A. and Johnson, C.C. (2004) Multiple risk factors for Parkinson's disease. *J. Neurol. Sci.*, **217**, 169–174.
5. Tanner, C.M., Ottman, R., Goldman, S.M., Ellenberg, J., Chan, P., Mayeux, R. and Langston, J.W. (1999) Parkinson disease in twins: an etiologic study. *JAMA*, **281**, 341–346.
6. Polymeropoulos, M.H., Lavedan, C., Leroy, E., Ide, S.E., Dehejia, A., Dutra, A., Pike, B., Root, H., Rubenstein, J., Boyer, R. *et al.* (1997) Mutation in the alpha-synuclein gene identified in families with Parkinson's disease. *Science*, **276**, 2045–2047.
7. Leroy, E., Boyer, R., Auburger, G., Leube, B., Ulm, G., Mezey, E., Harta, G., Brownstein, M.J., Jonnalagada, S., Chernova, T. *et al.* (1998) The ubiquitin pathway in Parkinson's disease. *Nature*, **395**, 451–452.
8. Kitada, T., Asakawa, S., Hattori, N., Matsumine, H., Yamamura, Y., Minoshima, S., Yokochi, M., Mizuno, Y. and Shimizu, N. (1998) Mutations in the parkin gene cause autosomal recessive juvenile parkinsonism. *Nature*, **392**, 605–608.
9. Bonifati, V., Rizzu, P., van Baren, M.J., Schaap, O., Breedveld, G.J., Krieger, E., Dekker, M.C., Squitieri, F., Ibanez, P., Joosse, M. *et al.* (2003) Mutations in the DJ-1 gene associated with autosomal recessive early-onset parkinsonism. *Science*, **299**, 256–259.
10. Valente, E.M., Abou-Sleiman, P.M., Caputo, V., Muqit, M.M., Harvey, K., Gispert, S., Ali, Z., Del Turco, D., Bentivoglio, A.R., Healy, D.G. *et al.* (2004) Hereditary early-onset Parkinson's disease caused by mutations in PINK1. *Science*, **304**, 1158–1160.
11. Singleton, A.B., Farrer, M., Johnson, J., Singleton, A., Hague, S., Kachergus, J., Hulihan, M., Peuralinna, T., Dutra, A., Nussbaum, R. *et al.* (2003) alpha-Synuclein locus triplication causes Parkinson's disease. *Science*, **302**, 841.
12. Hirsch, E., Graybiel, A.M. and Agid, Y.A. (1988) Melanized dopaminergic neurons are differentially susceptible to degeneration in Parkinson's disease. *Nature*, **334**, 345–348.
13. German, D.C., Manaye, K.F., Sonsalla, P.K. and Brooks, B.A. (1992) Midbrain dopaminergic cell loss in Parkinson's disease and MPTP-induced parkinsonism: sparing of calbindin-D28k-containing cells. *Ann. N Y Acad. Sci.*, **648**, 42-62.
14. Damier, P., Hirsch, E.C., Agid, Y. and Graybiel, A.M. (1999) The substantia nigra of the human brain. II. Patterns of loss of dopamine-containing neurons in Parkinson's disease. *Brain*, **122**, 1437–1448.
15. German, D.C., Manaye, K., Smith, W.K., Woodward, D.J. and Saper, C.B. (1989) Midbrain dopaminergic cell loss in Parkinson's disease: computer visualization. *Ann. Neurol.*, **26**, 507–514.
16. German, D.C., Dubach, M., Askari, S., Speciale, S.G. and Bowden, D.M. (1988) 1-Methyl-4-phenyl-1,2,3,6-tetrahydropyridine-induced parkinsonian syndrome in *Macaca fascicularis*: which midbrain dopaminergic neurons are lost? *Neuroscience*, **24**, 161–174.
17. Rodriguez, M., Barroso-Chinea, P., Abdala, P., Obeso, J. and Gonzalez-Hernandez, T. (2001) Dopamine cell degeneration induced by intraventricular administration of 6-hydroxydopamine in the rat: similarities with cell loss in parkinson's disease. *Exp. Neurol.*, **169**, 163–181.
18. Pakkenberg, B., Moller, A., Gundersen, H.J., Mouritzen Dam, A. and Pakkenberg, H. (1991) The absolute number of nerve cells in substantia nigra in normal subjects and in patients with Parkinson's disease estimated with an unbiased stereological method. *J. Neurol. Neurosurg. Psychiatry*, **54**, 30–33.
19. McGeer, P.L., Itagaki, S., Akiyama, H. and McGeer, E.G. (1988) Rate of cell death in parkinsonism indicates active neuropathological process. *Ann. Neurol.*, **24**, 574–576.
20. Fearnley, J.M. and Lees, A.J. (1991) Ageing and Parkinson's disease: substantia nigra regional selectivity. *Brain*, **114**, 2283–2301.
21. Javoy-Agid, F. and Agid, Y. (1980) Is the mesocortical dopaminergic system involved in Parkinson disease? *Neurology*, **30**, 1326–1330.
22. McRitchie, D.A., Cartwright, H.R. and Halliday, G.M. (1997) Specific A10 dopaminergic nuclei in the midbrain degenerate in Parkinson's disease. *Exp. Neurol.*, **144**, 202–213.
23. Yamada, T., McGeer, P.L., Baimbridge, K.G. and McGeer, E.G. (1990) Relative sparing in Parkinson's disease of substantia nigra dopamine neurons containing calbindin-D28K. *Brain Res.*, **526**, 303–307.
24. Parent, A., Fortin, M., Cote, P.Y. and Cicchetti, F. (1996) Calcium-binding proteins in primate basal ganglia. *Neurosci. Res.*, **25**, 309–334.
25. Liang, C.L., Sinton, C.M., Sonsalla, P.K. and German, D.C. (1996) Midbrain dopaminergic neurons in the mouse that contain calbindin-D28k exhibit reduced vulnerability to MPTP-induced neurodegeneration. *Neurodegeneration*, **5**, 313–318.
26. Schein, J.C., Hunter, D.D. and Roffler-Tarlov, S. (1998) Girk2 expression in the ventral midbrain, cerebellum, and olfactory bulb and its relationship to the murine mutation weaver. *Dev. Biol.*, **204**, 432–450.
27. Karschin, C., Dissmann, E., Stuhmer, W. and Karschin, A. (1996) IRK(1–3) and GIRK(1–4) inwardly rectifying K^+ channel mRNAs are differentially expressed in the adult rat brain. *J. Neurosci.*, **16**, 3559–3570.
28. Roffler-Tarlov, S., Martin, B., Graybiel, A.M. and Kauer, J.S. (1996) Cell death in the midbrain of the murine mutation weaver. *J. Neurosci.*, **16**, 1819–1826.
29. Liss, B., Neu, A. and Roeper, J. (1999) The weaver mouse gain-of-function phenotype of dopaminergic midbrain neurons is determined by coactivation of wvGirk2 and K-ATP channels. *J. Neurosci.*, **19**, 8839–8848.
30. Inanobe, A., Yoshimoto, Y., Horio, Y., Morishige, K.I., Hibino, H., Matsumoto, S., Tokunaga, Y., Maeda, T., Hata, Y., Takai, Y. *et al.* (1999) Characterization of G-protein-gated K^+ channels composed of Kir3.2 subunits in dopaminergic neurons of the substantia nigra. *J. Neurosci.*, **19**, 1006–1017.
31. Isacson, O. (1993) On neuronal health. *Trends Neurosci.*, **16**, 306–308.
32. Seo, H., Sonntag, K.C. and Isacson, O. (2004) Generalized brain and skin proteasome inhibition in Huntington's disease. *Ann. Neurol.*, **56**, 319–328.
33. McCaffery, P. and Drager, U.C. (1994) High levels of a retinoic acid-generating dehydrogenase in the meso-telencephalic dopamine system. *Proc. Natl Acad. Sci. USA*, **91**, 7772–7776.
34. Sirinathsinghji, D.J., Kupsch, A., Mayer, E., Zivin, M., Pufal, D. and Oertel, W.H. (1992) Cellular localization of tyrosine hydroxylase mRNA and cholecystokinin mRNA-containing cells in the ventral mesencephalon of the common marmoset: effects of 1-methyl-4-phenyl-1,2,3,6-tetrahydropyridine. *Brain Res. Mol. Brain Res.* **12**, 267–274.
35. Seroogy, K.B., Dangaran, K., Lim, S., Haycock, J.W. and Fallon, J.H. (1989) Ventral mesencephalic neurons containing both cholecystokinin- and tyrosine hydroxylase-like immunoreactivities project to forebrain regions. *J. Comp. Neurol.*, **279**, 397–414.
36. Draghici, S., Khatri, P., Martins, R.P., Ostermeier, G.C. and Krawetz, S.A. (2003) Global functional profiling of gene expression. *Genomics*, **81**, 98–104.
37. Seabra, M.C., Mules, E.H. and Hume, A.N. (2002) Rab GTPases, intracellular traffic and disease. *Trends Mol. Med.*, **8**, 23–30.
38. O'Connor, L., Strasser, A., O'Reilly, L.A., Hausmann, G., Adams, J.M., Cory, S. and Huang, D.C. (1998) Bim: a novel member of the Bcl-2 family that promotes apoptosis. *EMBO J.*, **17**, 384–395.

39. Tanaka, Y., Engelender, S., Igarashi, S., Rao, R.K., Wanner, T., Tanzi, R.E., Sawa, A., V, L.D., Dawson, T.M. and Ross, C.A. (2001) Inducible expression of mutant alpha-synuclein decreases proteasome activity and increases sensitivity to mitochondria-dependent apoptosis. *Hum. Mol. Genet.*, **10**, 919–926.
40. Przedborski, S., Tieu, K., Perier, C. and Vila, M. (2004) MPTP as a mitochondrial neurotoxic model of Parkinson's disease. *J. Bioenerg. Biomembr.*, **36**, 375–379.
41. Bayer, S.A., Triarhou, L.C., Thomas, J.D. and Ghetti, B. (1994) Correlated quantitative studies of the neostriatum, nucleus accumbens, substantia nigra, and ventral tegmental area in normal and weaver mutant mice. *J. Neurosci.*, **14**, 6901–6910.
42. Graybiel, A.M., Ohta, K. and Roffler-Tarlov, S. (1990) Patterns of cell and fiber vulnerability in the mesostriatal system of the mutant mouse weaver. I. Gradients and compartments. *J. Neurosci.*, **10**, 720–733.
43. Halestrap, A.P. and Brennerb, C. (2003) The adenine nucleotide translocase: a central component of the mitochondrial permeability transition pore and key player in cell death. *Curr. Med. Chem.*, **10**, 1507–1525.
44. Marzo, I., Brenner, C., Zamzami, N., Jurgensmeier, J.M., Susin, S.A., Vieira, H.L., Prevost, M.C., Xie, Z., Matsuyama, S., Reed, J.C. *et al.* (1998) Bax and adenine nucleotide translocator cooperate in the mitochondrial control of apoptosis. *Science*, **281**, 2027–2031.
45. Lu, T., Pan, Y., Kao, S.Y., Li, C., Kohane, I., Chan, J. and Yankner, B.A. (2004) Gene regulation and DNA damage in the ageing human brain. *Nature*, **429**, 883–891
46. Quesada, A. and Micevych, P.E. (2004) Estrogen interacts with the IGF-1 system to protect nigrostriatal dopamine and maintain motoric behavior after 6-hydroxdopamine lesions. *J. Neurosci. Res.*, **75**, 107–116.
47. Krishnamurthi, R., Stott, S., Maingay, M., Faull, R.L., McCarthy, D., Gluckman, P. and Guan, J. (2004) N-terminal tripeptide of IGF-1 improves functional deficits after 6-OHDA lesion in rats. *Neuroreport*, **15**, 1601–1604.
48. Wickman, K. and Clapham, D.E. (1995) Ion channel regulation by G proteins. *Physiol. Rev.*, **75**, 865–885.
49. Slesinger, P.A., Patil, N., Liao, Y.J., Jan, Y.N., Jan, L.Y. and Cox, D.R. (1996) Functional effects of the mouse weaver mutation on G protein-gated inwardly rectifying K^+ channels. *Neuron*, **16**, 321–331.
50. Palmieri, F. (2004) The mitochondrial transporter family (SLC25): physiological and pathological implications. *Pflugers Arch.*, **447**, 689–709.
51. Cassarino, D.S., Parks, J.K., Parker, W.D., Jr. and Bennett, J.P., Jr. (1999) The parkinsonian neurotoxin MPP+ opens the mitochondrial permeability transition pore and releases cytochrome c in isolated mitochondria via an oxidative mechanism. *Biochim. Biophys. Acta*, **1453**, 49–62.
52. Kiranadi, B., Bangham, J.A. and Smith, P.A. (1991) Inhibition of electrical activity in mouse pancreatic beta-cells by the ATP/ADP translocase inhibitor, bongkrekic acid. *FEBS Lett.*, **283**, 93–96.
53. Guan, J., Miller, O.T., Waugh, K.M., McCarthy, D.C. and Gluckman, P.D. (2001) Insulin-like growth factor-1 improves somatosensory function and reduces the extent of cortical infarction and ongoing neuronal loss after hypoxia-ischemia in rats. *Neuroscience*, **105**, 299–306.
54. Wang, J.M., Hayashi, T., Zhang, W.R., Sakai, K., Shiro, Y. and Abe, K. (2000) Reduction of ischemic brain injury by topical application of insulin-like growth factor-I after transient middle cerebral artery occlusion in rats. *Brain Res.*, **859**, 381–385.
55. Kermer, P., Klocker, N., Labes, M. and Bahr, M. (2000) Insulin-like growth factor-I protects axotomized rat retinal ganglion cells from secondary death via PI3-K-dependent Akt phosphorylation and inhibition of caspase-3 *in vivo*. *J. Neurosci.*, **20**, 2–8.
56. Poe, B.H., Linville, C., Riddle, D.R., Sonntag, W.E. and Brunso-Bechtold, J.K. (2001) Effects of age and insulin-like growth factor-1 on neuron and synapse numbers in area CA3 of hippocampus. *Neuroscience*, **107**, 231–238.
57. Vincent, A.M., Mobley, B.C., Hiller, A. and Feldman, E.L. (2004) IGF-I prevents glutamate-induced motor neuron programmed cell death. *Neurobiol. Dis.*, **16**, 407–416.
58. Zawada, W.M., Kirschman, D.L., Cohen, J.J., Heidenreich, K.A. and Freed, C.R. (1996) Growth factors rescue embryonic dopamine neurons from programmed cell death. *Exp. Neurol.*, **140**, 60–67.
59. Shavali, S., Ren, J. and Ebadi, M. (2003) Insulin-like growth factor-1 protects human dopaminergic SH-SY5Y cells from salsolinol-induced toxicity. *Neurosci. Lett.*, **340**, 79–82.
60. Strasburger, C.J., Bidlingmaier, M., Wu, Z. and Morrison, K.M. (2001) Normal values of insulin-like growth factor I and their clinical utility in adults. *Horm. Res.*, **55**(Suppl. 2), 100–105.
61. van Dam, P.S. and Aleman, A. (2004) Insulin-like growth factor-I, cognition and brain aging. *Eur. J. Pharmacol.*, **490**, 87–95.
62. Yegen, B.C. (2003) Bombesin-like peptides: candidates as diagnostic and therapeutic tools. *Curr. Pharm. Des.*, **9**, 1013–1022.
63. Cuttitta, F., Carney, D.N., Mulshine, J., Moody, T.W., Fedorko, J., Fischler, A. and Minna, J.D. (1985) Bombesin-like peptides can function as autocrine growth factors in human small-cell lung cancer. *Nature*, **316**, 823–826.
64. Alexander, R.W., Upp, J.R., Jr., Poston, G.J., Gupta, V., Townsend, C.M., Jr. and Thompson, J.C. (1988) Effects of bombesin on growth of human small cell lung carcinoma *in vivo*. *Cancer Res.*, **48**, 1439–1441.
65. Larsen, P.J., Saermark, T. and Mikkelsen, J.D. (1989) An immunohistochemical demonstration of gastrin-releasing peptide (GRP) in the rat substantia nigra. *J. Chem. Neuroanat.*, **2**, 83–93.
66. Goodman, E.C. and Iversen, L.L. (1986) Calcitonin gene-related peptide: novel neuropeptide. *Life Sci.*, **38**, 2169–2178.
67. Bell, D. and McDermott, B.J. (1996) Calcitonin gene-related peptide in the cardiovascular system: characterization of receptor populations and their (patho)physiological significance. *Pharmacol. Rev.*, **48**, 253–288.
68. Burvenich, S., Unsicker, K. and Krieglstein, K. (1998) Calcitonin gene-related peptide promotes differentiation, but not survival, of rat mesencephalic dopaminergic neurons *in vitro*. *Neuroscience*, **86**, 1165–1172.
69. Arimura, A. (1992) Pituitary adenylate cyclase activating polypeptide (PACAP): discovery and current status of research. *Regul. Pept.*, **37**, 287–303.
70. Ogi, K., Kimura, C., Onda, H., Arimura, A. and Fujino, M. (1990) Molecular cloning and characterization of cDNA for the precursor of rat pituitary adenylate cyclase activating polypeptide (PACAP). *Biochem. Biophys. Res. Commun.*, **173**, 1271–1279.
71. Vaudry, D., Gonzalez, B.J., Basille, M., Yon, L., Fournier, A. and Vaudry, H. (2000) Pituitary adenylate cyclase-activating polypeptide and its receptors: from structure to functions. *Pharmacol. Rev.*, **52**, 269–324.
72. Arimura, A. (1998) Perspectives on pituitary adenylate cyclase activating polypeptide (PACAP) in the neuroendocrine, endocrine, and nervous systems. *Jpn. J. Physiol.*, **48**, 301–331.
73. Reglodi, D., Lubics, A., Tamas, A., Szalontay, L. and Lengvari, I. (2004) Pituitary adenylate cyclase activating polypeptide protects dopaminergic neurons and improves behavioral deficits in a rat model of Parkinson's disease. *Behav Brain. Res.*, **151**, 303–312.
74. Takei, N., Skoglosa, Y. and Lindholm, D. (1998) Neurotrophic and neuroprotective effects of pituitary adenylate cyclase-activating polypeptide (PACAP) on mesencephalic dopaminergic neurons. *J. Neurosci. Res.*, **54**, 698–706.
75. Delgado, M. and Ganea, D. (2003) Neuroprotective effect of vasoactive intestinal peptide (VIP) in a mouse model of Parkinson's disease by blocking microglial activation. *FASEB J.*, **17**, 944–946.
76. Dogrukol-Ak, D., Tore, F. and Tuncel, N. (2004) Passage of VIP/PACAP/secretin family across the blood-brain barrier: therapeutic effects. *Curr. Pharm. Des.*, **10**, 1325–1340.
77. Greenamyre, J.T., Sherer, T.B., Betarbet, R. and Panov, A.V. (2001) Complex I and Parkinson's disease. *IUBMB Life*, **52**, 135–141.
78. Betarbet, R., Sherer, T.B., MacKenzie, G., Garcia-Osuna, M., Panov, A.V. and Greenamyre, J.T. (2000) Chronic systemic pesticide exposure reproduces features of Parkinson's disease. *Nat. Neurosci.*, **3**, 1301–1306.
79. Beal, M.F. (2004) Commentary on 'alpha-synuclein and mitochondria: a tangled skein'. *Exp. Neurol.*, **186**, 109–111.
80. Hsu, L.J., Sagara, Y., Arroyo, A., Rockenstein, E., Sisk, A., Mallory, M., Wong, J., Takenouchi, T., Hashimoto, M. and Masliah, E. (2000) alpha-synuclein promotes mitochondrial deficit and oxidative stress. *Am. J. Pathol.*, **157**, 401–410.
81. Palacino, J.J., Sagi, D., Goldberg, M.S., Krauss, S., Motz, C., Wacker, M., Klose, J. and Shen, J. (2004) Mitochondrial dysfunction and oxidative damage in parkin-deficient mice. *J. Biol. Chem.*, **279**, 18614–18622.

82. Graham, D.G. (1978) Oxidative pathways for catecholamines in the genesis of neuromelanin and cytotoxic quinones. *Mol. Pharmacol.*, **14**, 633–643.
83. Ciliax, B.J., Drash, G.W., Staley, J.K., Haber, S., Mobley, C.J., Miller, G.W., Mufson, E.J., Mash, D.C. and Levey, A.I. (1999) Immunocytochemical localization of the dopamine transporter in human brain. *J. Comp. Neurol.*, **409**, 38–56.
84. Haber, S.N., Ryoo, H., Cox, C. and Lu, W. (1995) Subsets of midbrain dopaminergic neurons in monkeys are distinguished by different levels of mRNA for the dopamine transporter: comparison with the mRNA for the D2 receptor, tyrosine hydroxylase and calbindin immunoreactivity. *J. Comp. Neurol.*, **362**, 400–410.
85. Uhl, G.R., Walther, D., Mash, D., Faucheux, B. and Javoy-Agid, F. (1994) Dopamine transporter messenger RNA in Parkinson's disease and control substantia nigra neurons. *Ann. Neurol.*, **35**, 494–498.
86. Aubert, I., Brana, C., Pellevoisin, C., Giros, B., Caille, I., Carles, D., Vital, C. and Bloch, B. (1997) Molecular anatomy of the development of the human substantia nigra. *J. Comp. Neurol.*, **379**, 72–87.
87. Willingham, S., Outeiro, T.F., DeVit, M.J., Lindquist, S.L. and Muchowski, P.J. (2003) Yeast genes that enhance the toxicity of a mutant huntingtin fragment or alpha-synuclein. *Science*, **302**, 1769–1772.
88. Hauser, M.A., Li, Y.J., Takeuchi, S., Walters, R., Noureddine, M., Maready, M., Darden, T., Hulette, C., Martin, E., Hauser, E. *et al.* (2003) Genomic convergence: identifying candidate genes for Parkinson's disease by combining serial analysis of gene expression and genetic linkage. *Hum. Mol. Genet.*, **12**, 671–677.
89. Grimm, J., Mueller, A., Hefti, F. and Rosenthal, A. (2004) Molecular basis for catecholaminergic neuron diversity. *Proc. Natl Acad. Sci. USA*, **101**, 13891–13896.
90. Livak, K.J. and Schmittgen, T.D. (2001) Analysis of relative gene expression data using real-time quantitative PCR and the 2(−Delta Delta C(T)) method. *Methods*, **25**, 402–408.
91. Zufferey, R., Dull, T., Mandel, R.J., Bukovsky, A., Quiroz, D., Naldini, L. and Trono, D. (1998) Self-inactivating lentivirus vector for safe and efficient *in vivo* gene delivery. *J. Virol.*, **72**, 9873–9880.